ANTIMICROBIAL AGENTS AND CHEMOTHERAPY, Dec. 1993, p. 2722–2726
0066-4804/93/122722-05$02.00/0

Vol. 37, No. 12

Electron Microscopic Study of the Effect of Zinc on *Tritrichomonas foetus*

MARLENE BENCHIMOL,* JOÃO CARLOS DE AQUINO ALMEIDA, ULYSSES LINS, NOÊMIA RODRIGUES GONÇALVES, AND WANDERLEY DE SOUZA

Laboratório de Ultraestrutura Celular Hertha Meyer, Instituto de Biofísica Carlos Chagas Filho, Universidade Federal do Rio de Janeiro, Ilha do Fundão, 21941-900, Rio de Janeiro, Brazil

Received 29 March 1993/Returned for modification 20 May 1993/Accepted 27 September 1993

At concentrations of 3.1 to 24 mM, zinc inhibits the multiplication of and kills the pathogenic protozoan *Tritrichomonas foetus*. Transmission electron microscopy showed that the hydrogenosome, a organelle which is involved in the metabolism of pyruvate and the site of formation of molecular hydrogen, constitutes the main site of the initial effect of zinc. The hydrogenosomal vesicle increases its electron density and dimension. Electron spectroscopy imaging and the electron energy loss spectrum showed the presence of zinc, calcium, and oxygen in the electron-dense areas of the hydrogenosome.

Infections caused by protozoa of the *Trichomonadidae* family, especially *Trichomonas vaginalis* and *Tritrichomonas foetus*, constitute important sexually transmitted diseases in humans and cattle, respectively. In both cases, proliferation of the parasites in the urogenital cavity of the female induces epithelial lesions, infertility, and even abortion (for a review, see reference 10). In the case of human trichomoniasis, infection of the male urinary tract is well established (10, 11). However, the frequency with which trichomonal infection is responsible for various clinical syndromes such as urethritis, prostatitis, balanitis, and epididymitis remains controversial (11, 21). Parasites have been found in the urethras of about 70% of men who had contact with heavily infected women within the preceding 48 h. However, this percentage significantly decreases after a few weeks, indicating that the male urinary tract inhibits parasite proliferation (21).

Prostatic secretion has been considered to play an essential role in the killing of infectious microorganisms of the male genitourinary tract (8, 20). It has been shown that this microbicidal effect is related to the concentration of zinc found in the prostatic fluid (8, 9, 15). In addition, it has been clearly shown that at concentrations similar to those found in healthy males (about 3.5 mM), zinc kills *T. vaginalis*. However, the mechanism of action of zinc in trichomonads has not been determined. In the present report we show, using transmission electron microscopy and electron spectroscopic imaging (ESI), that the hydrogenosome, a key organelle in the metabolism of trichomonads, is significantly affected by zinc.

MATERIALS AND METHODS

Microorganism. The strain of *T. foetus* used in the present study was isolated from the urogenital tract of a bull from the state of Rio de Janeiro, Brazil, and has been maintained in TYM Diamond's medium (7). The cells were cultivated for 30 h at 36.5°C, which corresponds to the end of the logarithmic phase of growth. The inoculum consisted of 10^5 cells per ml. After an initial growth for 12 h, $ZnSO_4$ at concentrations of 3.1, 6.2, 12, and 24 mM was added to the cultures. In some experiments, $ZnSO_4$ was added together with the inoculum. After incubation times that varied from 5 to 30 h, samples were collected for determination of cell density by using a Neubauer chamber and for electron microscopy, as described below.

Electron microscopy. Cells were collected by centrifugation (450 × *g* for 4 min at 4°C) and fixed for 2 h at room temperature in a solution containing 2.5% glutaraldehyde and 5 mM $CaCl_2$ in 0.1 M cacodylate buffer (pH 7.2). After fixation, the cells were washed in buffer and postfixed for 1 h at 4°C in 1% OsO_4, which was in 0.1 M cacodylate buffer plus 0.8% potassium ferrocyanide. Thereafter, the cells were washed in buffer, dehydrated in acetone, and embedded in Epon. Thin sections were stained with uranyl acetate and lead citrate and were examined in a Zeiss 900 electron microscope.

ESI. Very thin (<30 nm) sections of control and $ZnSO_4$-treated cells were collected on uncoated 400-mesh copper grids and were examined unstained with an accelerating voltage of 80 kV in a Zeiss CEM 902 electron microscope. The inelastically scattered electrons with element-specific energy losses were used to obtain high-resolution imaging of calcium, zinc, and oxygen distributions in the sections (1, 2, 19). A net distribution image for each element was obtained by computer-assisted image processing of the difference between an electron spectroscopic image taken just above the edge of the electron absorption specific for the element (Ca, 360 eV; Zn, 1,100 eV; oxygen, 550 eV) and a reference electron spectroscopic image taken below the edge (Ca, 330 eV; Zn, 1,000 eV; oxygen, 515 eV). The electron energy loss spectrum (ΔE) from the same region was also obtained in the ΔE region from 335 to 1,300 eV by using an energy acceptance window of approximately 5 eV.

RESULTS

Effect of Zn on cell growth. The addition of Zn together with the protozoa to a fresh culture medium significantly inhibited parasite proliferation (Fig. 1A), leading to its killing as evaluated by light microscopic observations. As expected, this effect was dependent on the Zn concentration. The addition of Zn 12 h after protozoan inoculation, at the beginning of the logarithmic phase of growth, also inhibited parasite division (Fig. 1B).

Transmission electron microscopy. The general structure of

* Corresponding author.

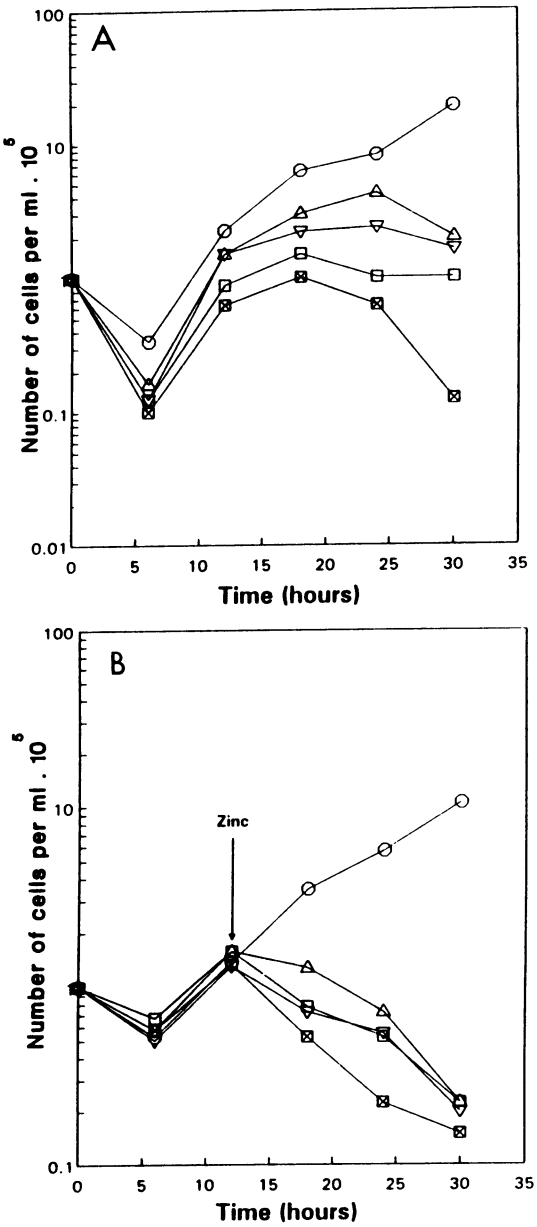

FIG. 1. Effect of $ZnSO_4$ on the growth of *T. foetus*. The presence of zinc significantly inhibits the growth of *T. foetus*. (A) Addition of zinc at the log phase. (B) Addition of zinc after 12 h. ○, control; △, 3.1 mM; ▽, 6.2 mM; □, 12 mM; ⊠, 24 mM.

T. foetus, as seen by transmission electron microscopy of thin sections, has been described in detail previously. Figure 2A shows a longitudinal section of an untreated protozoan displaying structures such as the nucleus, hydrogenosomes, axostyle, and glycogen particles. The hydrogenosome is surrounded by two closely adjacent unit membranes. In some regions there was a separation between the two membranes, so that a vesicle-like structure was formed in the intramembrane space. In some cases the electron density of this space was slightly lower than that of the hydrogenosome matrix (Fig. 2B).

In cells treated with Zn, the first morphological changes appeared in the hydrogenosome. Initially, the hydrogenosomal vesicle had a significantly increased electron density (Fig. 2C). Later, there was segregation of dense areas in the vesicle that were located especially at its periphery and in the central portion (Fig. 3A). In some advanced stages, observed after 30 h of incubation with all concentrations of Zn or after 15 min of incubation with higher concentrations of Zn, there was a significant increase in the area occupied by the hydrogenosomal vesicle, which occupied about 50% of the whole organelle (Fig. 3B). In these cases, the cytoplasm of the protozoan was also affected, with complete disorganization of the various structures. Digestive vacuoles rich in membranous materials and containing structures resembling hydrogenosomes were seen (Fig. 3C).

ESI. ESI analysis of untreated parasites has been described previously (6). When cells are fixed in the presence of Ca^{2+}, it was shown that this cation concentrates within the hydrogenosomal vesicle. Our present analysis with inelastically scattered electrons with Zn-specific energy losses showed that this element is concentrated in the electron-dense zone seen within the hydrogenosomal vesicle (Fig. 4A). Ca^{2+} (Fig. 4B) was also located within the vesicles, in the same areas where Zn was observed (Fig. 4C). In less dense areas, however, only Zn was observed. Oxygen was abundant in the whole vesicle.

The electron energy loss spectrum of the dense regions of the hydrogenosome showed peaks for calcium, oxygen, and zinc, showing unequivocally that the electron-dense reaction product seen in the hydrogenosome is due to the presence of calcium and zinc (Fig. 5).

DISCUSSION

It has been shown that the nucleus of mature spermatozoa contains zinc, in particular, in association with sulfur-rich structures, contributing to the stability of the quaternary structure of the chromatin (for a review, see reference 14). Zinc is found in the prostatic secretion and apparently is involved in the process of antimicrobial defenses of the male genitourinary tract (8, 9, 15, 20).

Our present observations confirm those of previous studies (12, 13) showing that at concentrations found in the human prostatic secretion, Zn kills trichomonads. The previous investigators (12, 13) added Zn together with the trichomonads into the culture medium. We also showed that Zn inhibits parasite proliferation and parasites them even when it is added to cultures of organisms in the logarithmic phase of growth.

The analysis by transmission electron microscopy of trichomonads incubated in the presence of Zn showed that the hydrogenosome constitutes the main site of the initial effect of this cation. It is concentrated within the hydrogenosomal vesicle, a structure which is formed by the separation of the two membranes which enclose the hydrogenosome and which usually are closely adjacent. The electron density of the vesicle and the area it occupies in the hydrogenosome gradually increase. Electron spectroscopic imaging and the electron energy loss spectrum of hydrogenosomes of Zn-treated parasites showed clearly that this cation concentrates into the hydrogenosomal vesicle in the same regions which concentrate Ca^{2+}.

Previous cytochemical studies have shown that the hydrogenosome is an organelle involved in the uptake of cytoplasmic Ca^{2+}, which concentrates within the hydrogenosomal vesicle (3–5). It is important to point out that members of the *Trichomonadidae* family are anaerobic parasites which do not have a mitochondrion. The hydrogenosome, however,

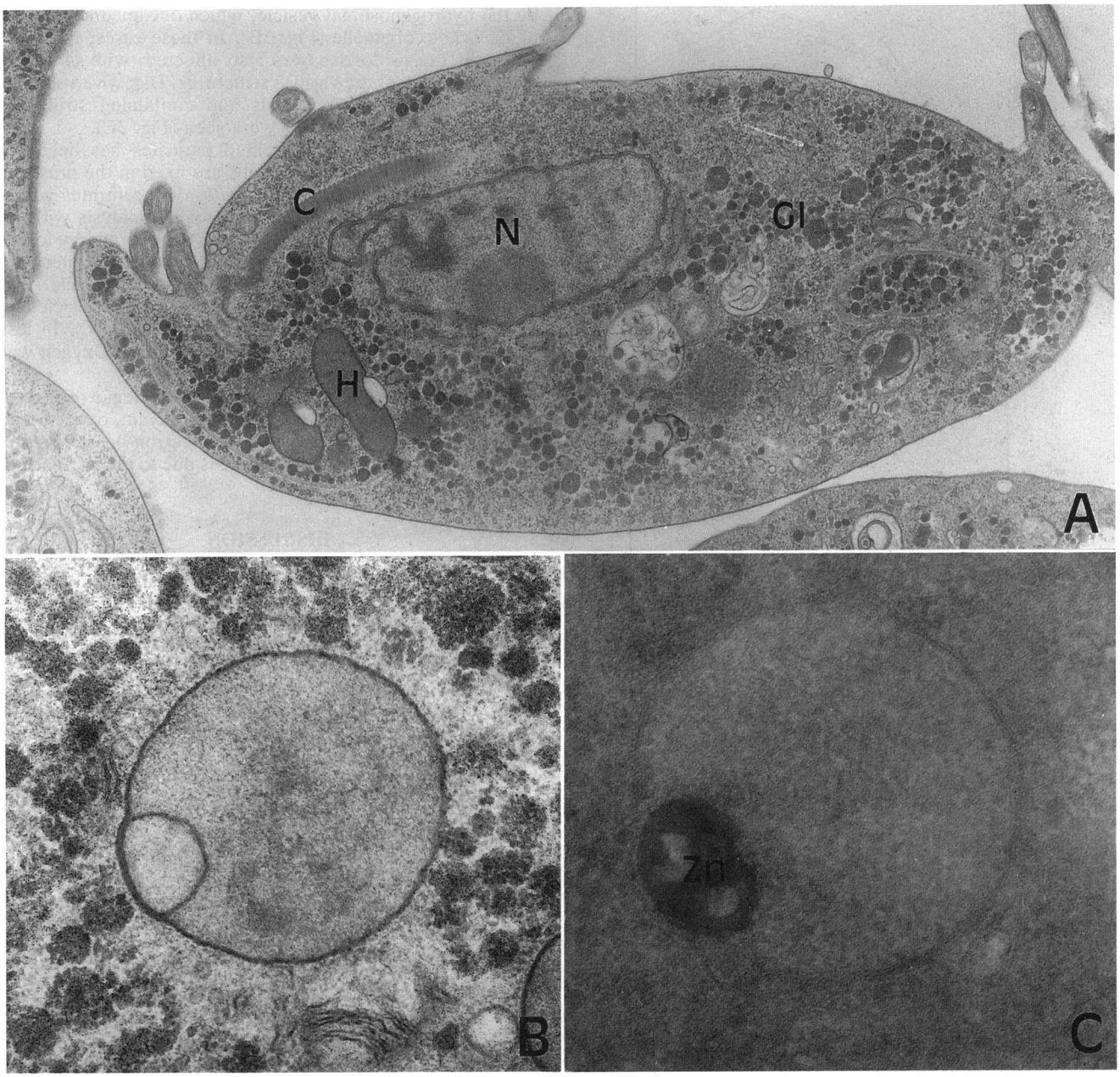

FIG. 2. (A) General view of an untreated *T. foetus* isolate showing the nucleus (N), costae (C), hydrogenosomes (H), and glycogen granules (Gl). Magnification, ×19,250. (B) Aspect of a hydrogenosome of a control cell. No dense material is seen within its flat vesicle. Magnification, ×50,000. (C) Hydrogenosome and its flat vesicle presenting electron-dense material after treatment with 3.1 mM $ZnSO_4$ (Zn). Magnification, ×127,500.

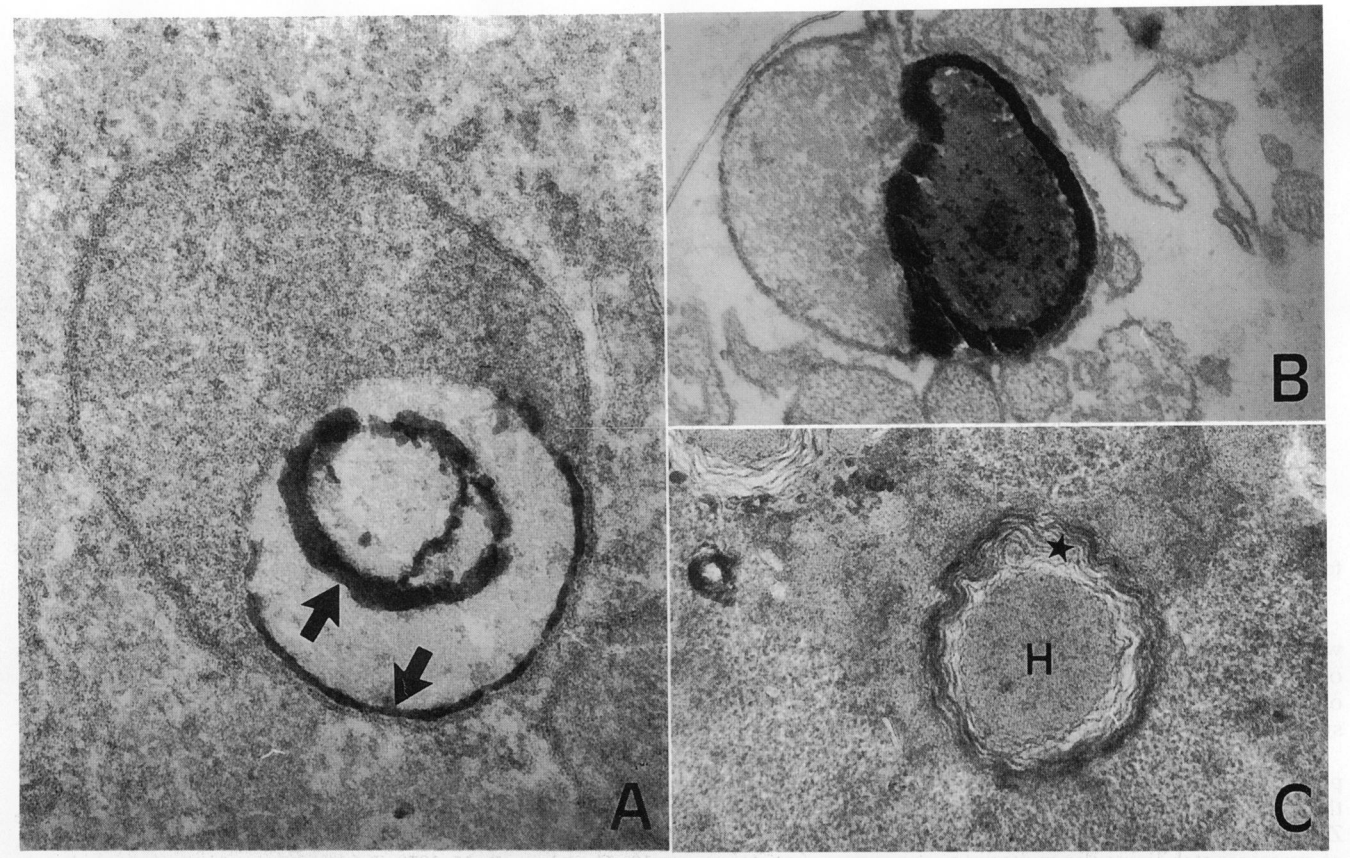

FIG. 3. (A) Reaction product (arrows) at hydrogenosome's flat vesicle after incubation with 3.1 mM $ZnSO_4$ for 24 h (arrows). Magnification, ×127,500. (B) Aspect of a hydrogenosome and cytoplasm of *T. foetus* after incubation with high concentrations of $ZnSO_4$ (12 mM) for 24 h. The cellular matrix presents signals of degeneration, and the hydrogenosome presents a strong reaction. Magnification, ×100,000. (C) Aspect of a digestive vacuole presenting myelin-like figures surrounding (star) a hydrogenosome-like structure (H). Magnification, ×50,000.

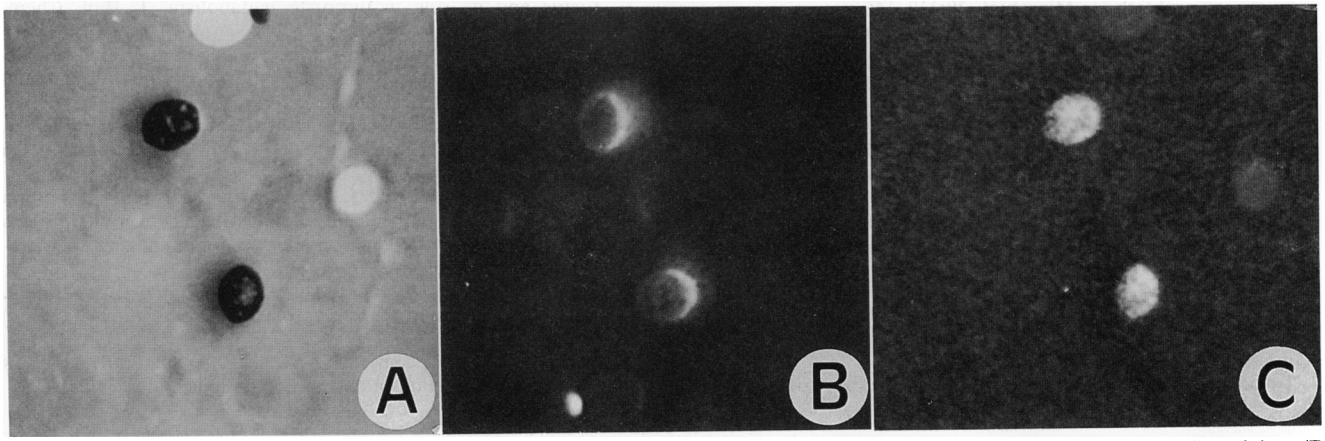

FIG. 4. (A) Zero-loss filtered image of two hydrogenosome vesicles from a Zn-treated (3.1 mM for 24 h) *T. foetus* cell. The calcium (B) and zinc (C) distribution images of the same vesicles in panel A indicate the colocalization of the two elements. Magnification, ×45,000.

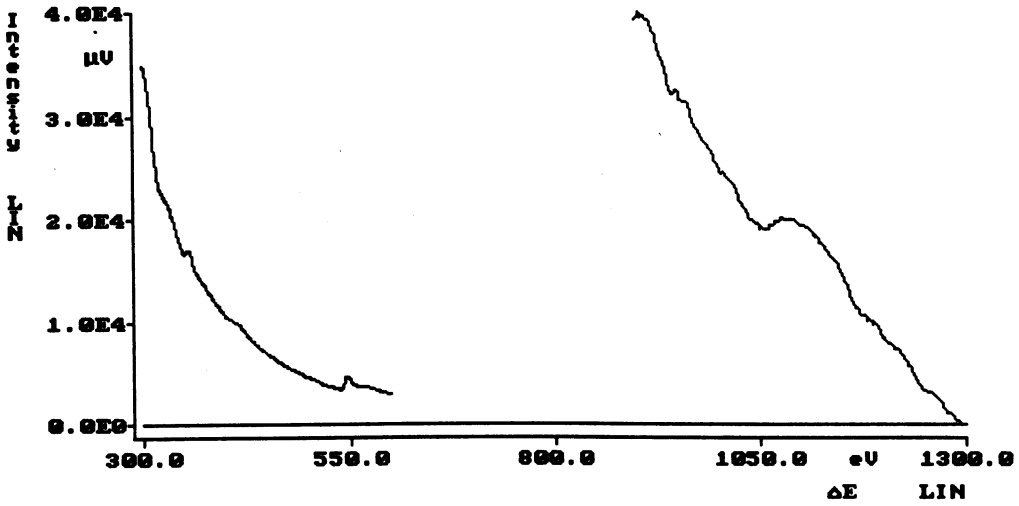

FIG. 5. Electron energy loss spectrum of a hydrogenosome's flat vesicle from a Zn-treated (3.1 mM for 24 h) *T. foetus* cell showing peaks for calcium (ΔE = 346 eV), oxygen (ΔE = 532 eV), and zinc (ΔE = 1,020 eV).

which presents enzymes that participate in the metabolism of the pyruvate formed in glycolysis, is the site of formation of molecular hydrogen and presents a cyanide-insusceptible superoxide dismutase (16–18).

On the basis of the observations presented above, it is possible that Zn is concentrated into the hydrogenosome by the same mechanisms involved in the uptake of Ca^{2+}. The Zn could, then, by its ability to interact with the thiol groups of cysteine, stabilizing the quaternary structures of proteins, interfere with the function of the hydrogenosome, an organelle which plays an important role in the metabolism of the parasite (for a review, see reference 18). Further biochemical studies are necessary to clarify the mechanism by which Zn kills the trichomonads.

ACKNOWLEDGMENTS

This work was supported by Financiadora de Estudos e Projetos and Conselho Nacional de Desenvolvimento Científico e Tecnológico.

REFERENCES

1. **Bauer, R.** 1988. Electron spectroscopic-imaging: an advanced technique for imaging and analysis in transmission electron microscopy. Methods Microbiol. **20:**113–146.
2. **Bauer, R., U. B. Hezal, and R. P. Partsch.** 1985. Electron spectroscopic imaging (ESI), an innovation method for image improvement, contrast enhancement and high resolution imaging of element distribution in transmission electron microscopy. Mikrosk. Elektronenmikrosk. **2**(Suppl.):26–35.
3. **Benchimol, M., and W. De Souza.** 1983. Fine structure and cytochemistry of the hydrogenosome of *Tritrichomonas foetus*. J. Protozool. **30:**422–425.
4. **Benchimol, M., C. A. Elias, and W. De Souza.** 1982. Ultrastructural localization of calcium in the plasma membrane and in the hydrogenosome. Exp. Parasitol. **54:**277–284.
5. **Chapman, A., A. O. C. Hann, D. Lindstead, and D. Lloyd.** 1985. Energy dispersive X-ray microanalysis of membrane-associated inclusions in hydrogenosomes isolated from *Trichomonas vaginalis*. J. Gen. Microbiol. **131:**2933–2939.
6. **De Souza, W., and M. Benchimol.** 1988. Electron spectroscopic imaging of calcium in the hydrogenosomes of *Tritrichomonas foetus*. J. Submicroscop. Cytol. Pathol. **20:**619–621.
7. **Diamond, L. S.** 1957. The establishment of various trichomonads of animals and man in axenic cultures. J. Parasitol. **43:**488–490.
8. **Fair, W. R., J. Couch, and N. Wehner.** 1976. Prostatic antibacterial factor: identity and significance. Urology **7:**169–177.
9. **Fair, W. R., and N. Wehner.** 1981. Further observations of the antibacterial nature of prostatic fluid. Infect. Immun. **3:**494–495.
10. **Honigberg, B. M.** 1978. Trichomonads of importance in human medicine, p. 275–454. *In* J. P. Kreier (ed.), Parasitic protozoa. Academic Press, Inc., New York.
11. **Krieger, J. N.** 1981. Urologic aspect of trichomoniasis. Invest. Urol. **18:**411–417.
12. **Krieger, J. N., and M. F. Rein.** 1982. Canine prostatic secretion kills *Trichomonas vaginalis*. Infect. Immun. **37:**77–81.
13. **Krieger, J. N., and M. F. Rein.** 1982. Zinc sensitivity of *Trichomonas vaginalis*: in vitro studies and clinical implications. J. Infect. Dis. **146:**341–345.
14. **Kvist, U., L. Bjorndahl, and S. Kjellberg.** 1987. Sperm nuclear zinc, chromatin stability, and male fertility. Scann. Mic. **1:**1241–1247.
15. **Levy, B. J., and W. R. Fair.** 1973. The location of antibacterial activity in the rat prostatic secretions. Invest. Urol. **11:**173–177.
16. **Lindmark, O. F., and M. Muller.** 1973. Hydrogenosome, a cytoplasmic organelle of the anaerobic flagellate *Trichomonas foetus* and its role in pyruvate metabolism. J. Biol. Chem. **248:**7724–7728.
17. **Muller, M.** 1975. Biochemistry of protozoan microbodies: peroxisomes, β-glycerophosphate oxidase bodies, hydrogenosomes. Annu. Rev. Microbiol. **29:**467–483.
18. **Muller, M.** 1990. Biochemistry of *Trichomonas vaginalis*, p. 53–83. *In* B. M. Honigberg (ed.), Trichomonads parasitic in humans. Springer-Verlag, New York.
19. **Ottensmeyer, F. P., and J. W. Andrew.** 1980. High resolution microanalysis of biological specimens by electron energy loss spectroscopy and by electron spectroscopic imaging. J. Ultrastruct. Res. **72:**336–348.
20. **Stamey, T. A., W. R. Fair, M. M. Timothy, and H. K. Chung.** 1968. Antibacterial nature of prostatic fluid. Nature (London) **218:**444–447.
21. **Weston, T. E. T., and C. S. Nicol.** 1963. Natural history of trichomonal infection in males. Br. J. Vener. Dis. **39:**251–257.